ADVANCED FUNCTIONAL MATERIALS
www.afm-journal.de

Co-deposited Cu(I) Complex for Tri-layered Yellow and White Organic Light-Emitting Diodes

Xiaochen Liu, Tao Zhang, Tianchi Ni, Nan Jiang, Zhiwei Liu,* Zuqiang Bian,* Zhenghong Lu, and Chunhui Huang*

Four compounds 4-[3,6-di(carbazol-9-yl)carbazol-9-yl]isoquinoline (TCIQ), 3-[3,6-di(carbazol-9-yl)carbazol-9-yl]pyridine (TCPy), 4-(carbazol-9-yl)isoquinoline (4CIQ), and 3-(carbazol-9-yl)pyridine (CPy) containing pyridyl or isoquinolyl were designed and synthesized to co-deposition with copper iodide (CuI) to form luminescent Cu(I) complex doped film in situ, which could be utilized as the emissive layer in organic light-emitting diodes (OLEDs). It is found that simple tri-layered yellow and white OLEDs can be achieved by co-depositing CuI and TCIQ with tuning ratios. The compound TCIQ serves a dual role as both a ligand for forming the emissive Cu(I) complex and as a host matrix for the formed emitter in yellow OLEDs, and a third role as a blue emitter in white OLEDs.

1. Introduction

Ever since the reports of multi-colour organic light-emitting diode (OLED) and polymer OLED (PLED),[1] OLEDs have attracted much attention due to their great potential applications in next-generation, large-area solid-state lighting. Up to now, many concepts have been developed to achieve a white OLED (WOLED): for example, i) stacked or pixelated OLED where each unit has different emission colors,[2] ii) single emitter based WOLED,[3] iii) blue OLED with external or internal down-conversion layers,[4] iv) OLED with single emission layers comprising all emitter molecules,[5] and v) single WOLED comprising an emissive layer containing different sub-layers for red, green and blue.[6] Among which, a hybrid approach that using singlet blue emitter and triplet red and green (or yellow) emitters harvests all excitons, as well as makes use of longer lived fluorescent blue, is potential to fabricate WOLEDs with better lifetime and simple device structure.[7]

While developing the architecture to improve efficiency, reducing the cost of WOLEDs is also important since materials cost is a major factor in mass production for future lighting market. Currently, most of the widely used red and green (or yellow) emitters are based on the complexes of noble metals such as Ir, Pt, which can generate light from both singlet and triplet excitons, thereby achieving nearly 100% internal quantum efficiency (IQE).[8] Unfortunately, the use of noble metal in an OLED greatly increases its cost, presenting a significant barrier to commercialization. So the inexpensive, abundant and environmentally friendly Cu(I) complexes are of much interest.[9] In addition, as a phosphorescence material, Cu(I) complex could theoretically reach the 100% IQE as well as noble metal complex, with which the efficiency of OLEDs reached today is as high as, or even higher than, those of highly efficient inorganic LEDs.[10] Therefore, Cu(I) complexes are considered as one of the most promising emitters for OLEDs.

Theoretically, an inexpensive WOLED with better lifetime and simple architecture could be fabricated by the combination of a blue fluorescence material and a yellow emissive Cu(I) complex. Nevertheless, researches were limited in photoluminescence (PL) studies of Cu(I) complexes for a long time, mainly because the PL quantum yield (PLQY) of early reported Cu(I) complexes are very low.[9d,11] Until recently, Cu(I) complexes with high PLQY and rich emission colour have been demonstrated, which shows a great potential in application in OLEDs.[12] Among Cu(I) complexes, $(CuX)_mL_n$ (X = I, Br, or Cl; L = pyridine derivatives) are well-known for their structural diversity, rich photophysical behavior, and high PLQY.[13] However, most of them have difficulties in fabricating OLEDs with traditional vacuum deposition method, due to their poor thermal stability. Until a co-deposition method has been demonstrated,[14] $(CuX)_mL_n$ could be used as emitters in OLEDs.

In this work, four compounds 4-[3,6-di(carbazol-9-yl)-carbazol-9-yl]isoquinoline (TCIQ), 3-[3,6-di(carbazol-9-yl) carbazol-9-yl]pyridine (TCPy), 4-(carbazol-9-yl)isoquinoline

X. C. Liu, T. C. Ni, Prof. Z. W. Liu, Prof. Z. Q. Bian, Prof. C. H. Huang
Beijing National Laboratory for Molecular Sciences (BNLMS)
State Key Laboratory of Rare Earth Materials Chemistry and Applications
College of Chemistry and Molecular Engineering
Peking University
Beijing 100871, PR China
E-mail: zwliu@pku.edu.cn; bianzq@pku.edu.cn
T. Zhang, Prof. N. Jiang, Prof. Z. H. Lu
Department of Physics
Yunnan University
2 Cuihu Bei Lu, Kunming 650091, PR China
E-mail: jiangnan@ynu.edu.cn
Prof. Z. H. Lu
Department of Materials Science and Engineering
University of Toronto
184 College Street, Toronto, Ontario, Canada, M5S 3E4

DOI: 10.1002/adfm.201400685

(4CIQ), and 3-(carbazol-9-yl)pyridine (CPy) containing pyridyl or isoquinolyl were synthesized. These compounds were designed to co-deposit with CuI to form luminescent Cu(I) complex doped emissive film in situ, and thus could be utilized as the emissive layer in OLEDs. By systematically studying these compounds and their co-deposited CuI:L (L = TCIQ, TCPy, 4CIQ, or CPy) films, it is found that the co-deposited CuI:TCIQ films can show pure yellow emission at a proper CuI doping concentration, while the compound TCIQ itself shows a blue emission, which enables us to make both yellow and white OLEDs. As a result, pure yellow electroluminescence (EL) at around 580 nm was observed at a CuI doping concentration of 5.0 wt%, while a series of WOLEDs with the best CIE colour coordinates of (0.30, 0.32) and color rendering index (CRI) of 89 were obtained by controlling the CuI concentration below 1.0 wt%.

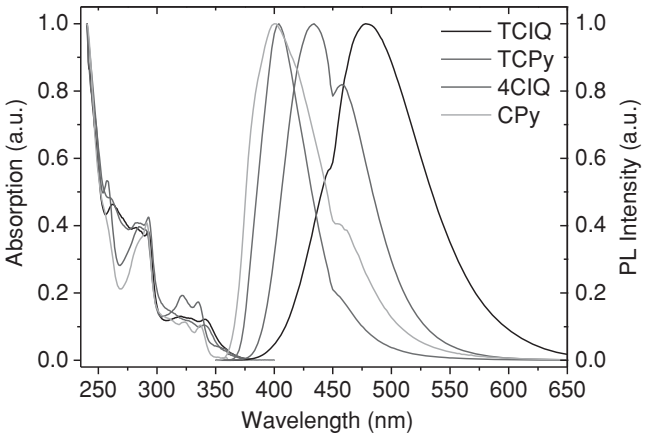

Figure 1. UV–vis absorption and PL spectra of TCIQ, TCPy, 4CIQ, and CPy in CH_2Cl_2 (10^{-5} M) at room temperature.

2. Results and Discussion

2.1. Synthesis and Characterization

The synthetic routes and chemical structures of TCIQ, TCPy, 4CIQ, and CPy are depicted in **Scheme 1**. The compounds were prepared through Ullmann coupling reaction of the corresponding bromide precursor with carbazole, purified by flash column chromatography on silica gel and subsequently twice thermal gradient sublimations. The characterization of the four compounds was established on the basis of ^{1}H NMR spectroscopy, mass spectrometry, and elemental analysis. Details are presented in the Experimental Section.

2.2. Photophysical Properties of Ligands

The room temperature absorption and emission spectra of TCIQ, TCPy, 4CIQ, and CPy were studied in CH_2Cl_2. As shown in **Figure 1** and **Table 1**, four compounds show similar patterns with four absorption bands centered between 250–350 nm. The peak absorption at around 290 nm can be identified to the carbazole-centered π–π^* transitions, while the peak in the range of 320–350 nm can be assigned to π–π^* transitions between the carbazole unit and the pyridyl or isoquinolyl.[15]

The maximum PL peaks of TCIQ, TCPy, 4CIQ, and CPy in solution are 478, 404, 434, and 401 nm, respectively. Red shifts were found when replacing pyridyl to isoquinolyl and introducing carbazolyl to the 3, 6 positions of carbazole. Based on density functional theory (DFT) calculations, the highest occupied molecular orbitals (HOMOs) of the four compounds are mainly located at the carbazolyl, while the lowest unoccupied molecular orbitals (LUMOs) are mainly distributed on the heterocyclic arylene (Figure S1, Supporting Information). The lower laying LUMO level was obtained by extending pyridyl to isoquinolyl, as well as the higher laying HOMO level obtained by introducing donor group on carbazole lead to a red shift in PL spectrum.

For application as a host material the triplet energy level is mainly considered for efficient energy transfer from host material to emitter.[8a] **Figure 2** shows PL spectra of TCIQ, TCPy, 4CIQ, and CPy in 2-MeTHF at 77 K. The triplet energy levels estimated from the low temperature PL spectra follow the sequence of TCIQ (2.6 eV) ≈ 4CIQ (2.6 eV) < TCPy (3.0 eV) ≈ CPy (3.0 eV). Apparently, the difference of triplet energy levels between TCIQ and 4CIQ is small as well as these between

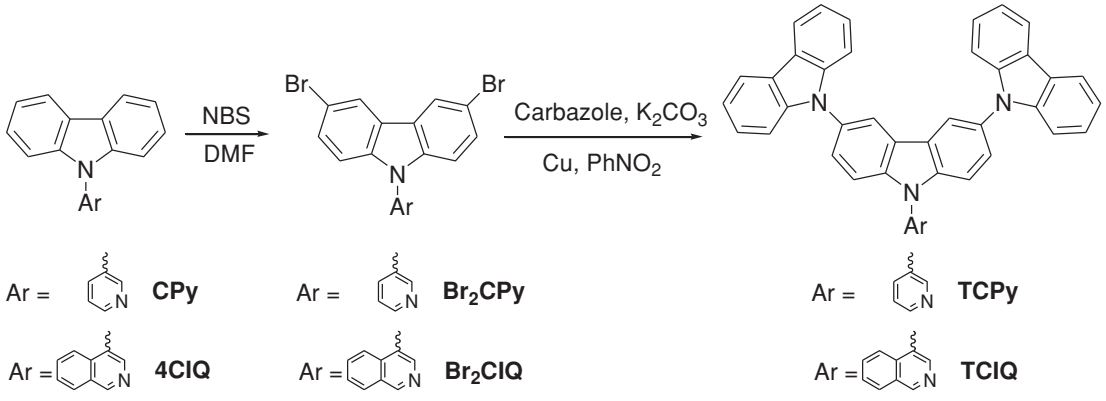

Scheme 1. Synthetic routes to TCIQ, TCPy, 4CIQ, and CPy.

Table 1. The photophysical, thermal, electrochemical and properties of TCIQ, TCPy, 4CIQ, and CPy.

Compound	λ_{abs} [nm]	E_g [eV]	λ_{em} [nm]	E_T [eV]	T_g/T_s [°C]	HOMO/LUMO [eV]
TCIQ	263, 293, 320, 343	3.3	478	2.6	186/453	5.9/2.6
TCPy	261, 293, 330, 343	3.3	404	3.0	163/431	5.7/2.4
4CIQ	258, 288, 320, 335	3.3	434	2.6	37/252	6.1/2.8
CPy	258, 290, 324, 338	3.4	401	3.0	– /225	6.0/2.6

TCPy and CPy. This reveals that the carbazolyl on the 3, 6 positions has almost no impact on the triplet energy. However, the triplet energy levels of TCIQ and 4CIQ are much lower than those of TCPy and CPy, which is caused by the expansion of conjugation system from pyridyl to isoquinolyl.

2.3. Thermal Properties

The thermal properties of the four compounds TCIQ, TCPy, 4CIQ, and CPy were determined by thermogravimetric analysis (TGA) and differential scanning calorimetry (DSC) (Table 1, Figures S2,S3, Supporting Information). As shown in Table 1, the sublimation temperature (T_s, corresponding to ~5% weight loss as analyzed by the software) and glass transition temperature (T_g) of TCIQ and TCPy are much higher than those of 4CIQ and CPy, which is because of larger molecular weights, as well as an introduction of carbazolyl to the 3, 6 positions of carbazole that makes the molecular configuration a non-planar structure.[16] Moreover, the T_g of 186 °C and 163 °C for the compounds TCIQ and TCPy, respectively, are significantly higher than that of widely used 4,4′-N,N′-dicarbazole-biphenyl (CBP) (62 °C)[17] and 1,3-bis(9-carbazolyl)benzene (mCP) (60 °C).[18] The relatively high T_g and T_s values make TCIQ and TCPy potential host materials for fabrication stable and high efficiency OLEDs by vacuum thermal evaporation technology.

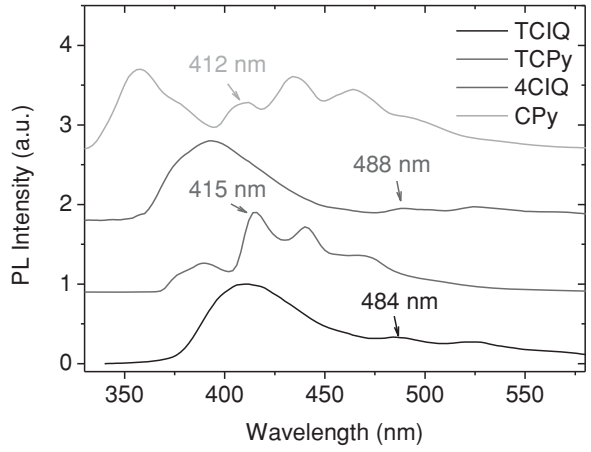

Figure 2. PL spectra of TCIQ, TCPy, 4CIQ, and CPy in 2-MeTHF (10^{-5} M) at 77 K.

2.4. Electrochemical Properties

The electrochemical properties of the four compounds were studied through cyclic voltammetry. In particular, the oxidation process was investigated in CH_2Cl_2 solution with ferrocene as an external or internal standard. All compounds exhibit irreversible oxidation waves like most carbazole derivatives (Figure S4, Supporting Information). Hence, the HOMO levels of the four compounds were roughly estimated by using a empirical formula,[19] which are 5.9, 5.7, 6.1 and 6.0 eV for TCIQ, TCPy, 4CIQ and CPy, respectively. The LUMO energy levels were deduced from HOMO energy levels and optical band gaps (Table 1) estimated by the onset of UV absorption, which are 2.6, 2.4, 2.8, and 2.6 eV for TCIQ, TCPy, 4CIQ and CPy, respectively.

Based on the cyclic voltammetry data, the HOMO energy levels of TCIQ and TCPy are found to be higher than that of 4CIQ and CPy, respectively. This is due to that the additional *+I*-effect on the carbazole by the carbazolyl substitution in the 3,6-positions of the carbazole unit will shift the HOMO levels to a higher value. Also, the change from pyridyl to isoquinolyl would cause a decrease in both the LUMO energy level and the HOMO energy level, owing to the expanded conjugated system that renders the electron density deficient in carbazoles. These cyclic voltammetry result reveals that TCIQ and TCPy with reduced hole injection barrier are much more suitable for use both as a hole injection layer and as a host layer.

2.5. Photophysical Properties of Co-deposited Films

The four compounds were designed as ligand with pyridyl or isoquinolyl that can react with CuI to form luminescent Cu(I) complex doped emissive film in situ during the co-deposition process, which could be utilized as the emissive layer in OLEDs. Prior to fabricating any OLEDs, a comprehensive photophysical investigation including PL spectrum, PLQY and decay lifetime of excited state has been conducted on the neat ligand films and co-deposited CuI:L (L = TCIQ, TCPy, 4CIQ or CPy) films with different CuI doping concentrations. **Figure 3** and **Table 2** displays PL spectra and photophysical data of all films.

All neat ligand films exhibit a fluorescent emission with maximum band in the range of 410–440 nm and decay lifetime in nanoseconds scale, while the co-deposited CuI:L films mainly have two emission peaks: a shorter one (410–440 nm) that arising from ligand and a longer one (≈560 nm for L = TCIQ or 4CIQ, ≈520 nm for L = TCPy or CPy) with decay lifetime in microseconds scale that proposed to be transition from in situ formed Cu(I) complex.[14] The relative intensity of the two peaks depends on the CuI doping concentration. For example, pure blue emission with a maximum emission band at 428 nm was observed in neat TCIQ film (i.e. CuI doping concentration of 0 wt%), white emission comprising both blue (436 nm) and yellow (562 nm) transitions was observed with a CuI doping concentration of 1.3 wt%, yellow emission was observed with a high CuI doping concentration of 7.1 wt%. It is interesting to note that the CuI:TCIQ film showed rich emission colors and could be used to fabricate colorful OLEDs.

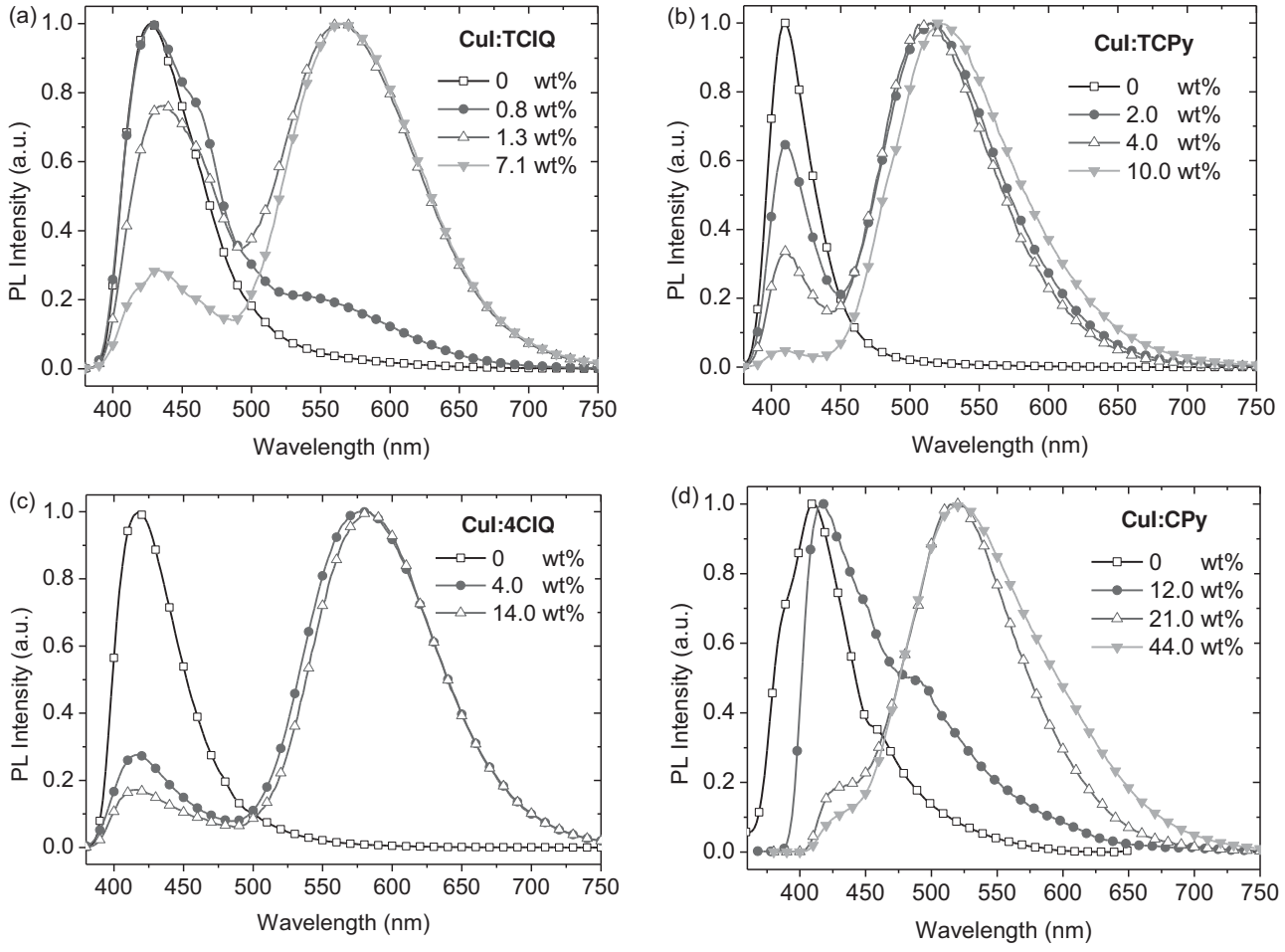

Figure 3. PL spectra of the neat ligand films and co-deposited CuI:L films. a) L = TCIQ, b) L = TCPy, c) L = 4CIQ, and d) L = CPy.

By examining the co-deposited films, it is found that the isoquinolyl based (CuI:TCIQ or CuI:4CIQ) film shows red-shift in the maximum PL wavelength by 40 nm as compared with that of the pyridyl based (CuI:TCPy or CuI:CPy) film, which shows a maximum PL wavelength around 520 nm. According to previous experimental and computational studies,[13a,20] excited states in the $(CuX)_mL_n$ complexes have been proposed to be halide-to-ligand charge transfer (XLCT), metal-to-ligand charge transfer (MLCT), and/or halide-to-metal charge transfer (XMCT) states. DFT calculation shows that the HOMOs are mainly distributed on the CuX center, while the LUMOs are concentrated on the ligands.[12c] Therefore, modifying the ligands mainly changes the LUMOs of the complexes, while keeps the HOMOs unchanged. Thus the red-shifted emission could be attributed to an extension of the conjugated system from pyridyl to isoquinolyl, which lowers the LUMOs energy level.

It is found that the co-deposited CuI:TCIQ and CuI:TCPy films are more efficient as emitters than are CuI:4CIQ and CuI:CPy films, respectively. Moreover, the PLQY of CuI:4CIQ and CuI:CPy films decreases quickly with the increasing concentration of ligand. These may be explained by a rigidochromic effect since TCIQ or TCPy has identical triplet energy level for energy transfer between the ligand and its in situ formed Cu(I) complex to that of 4CIQ or CPy, respectively. For TCIQ and TCPy, the substitution of a rigid carbazolyl on the 3,6-position of carbazole increases the rigidity of the ligands and thus restrains the structure change of Cu(I) complex upon photoexcitation, and consequently improves the efficiency of the co-deposited films.[9]

2.6. Electroluminescence Studies

Based on aforementioned studies, the compounds TCIQ and TCPy are found superior to its analogue compounds 4CIQ and CPy, respectively, in terms of high thermal stability, high glass transition temperature, and high PLQY of the co-deposited CuI:L films. These parameters are critical for material application in OLEDs. Moreover, the co-deposited CuI:TCIQ films showed yellow or white emission that differ from CuI:TCPy films (mainly green emission around 520 nm), which have attracted our interest and been further characterized in OLEDs. Consequently, all OLEDs were fabricated with a structure of ITO/MoO_3 (1 nm)/CBP (35 nm)/CuI:TCIQ (20 nm)/1,3,5-tris(N-phenylbenzimidazole-2-yl)benzene (TPBi, 65 nm)/LiF (1 nm)/Al, where CBP and TPBi are used as the hole and electron transporting layer, respectively. **Figure 4** shows the

Table 2. The maximum PL wavelength, PLQY and PL decay lifetime data of the neat ligand (L = TCIQ, TCPy, 4CIQ, or CPy) films and the co-deposited CuI:L films with different CuI doping concentrations.

Films	CuI Conc. [%]	λ_{em} [nm]	PLQY [%]	Lifetimes [μs]
CuI:TCIQ	0	428	22	0.0098, 0.0034
	0.8	428, 560	28	53.9, 16.3
	1.3	436, 562	26	4.0, 16.2
	7.1	433, 566	19	4.0, 15.4
CuI:TCPy	0	410	23	0.0052
	2.0	410, 516	42	4.1, 11.2
	4.0	410, 513	39	3.9, 10.5
	10.0	408, 522	29	2.6, 9.4
CuI:4CIQ	0	418	34	0.0089
	4.0	416, 580	10	1.4, 3.8
	14.0	415, 584	13	0.7, 2.5
CuI:CPy	0	411	8	0.0051
	12.0	416, 503	5	2.1, 5.6
	21.0	427, 519	13	2.3, 7.3
	44.0	427, 522	28	3.7, 11.1

schematic device structure, chemical structure, and energy level diagrams of the molecules.

The first set of OLEDs was fabricated to have a CuI doping concentration of 0 wt% (device **1**), 1.0 wt% (device **2**), 2.0 wt% (device **3**), and 5.0 wt% (device **4**), respectively. **Figure 5** are the EL spectra, current density–voltage (*CD–V*), luminance–voltage (*L–V*), current efficiency-luminance (*CE–L*), power efficiency–luminance (*PE–L*), and external quantum efficiency–current density (*EQE-CD*) characteristics of these four devices. The devices **2**, **3**, and **4** showed bright yellow emission with a maximum band around 580 nm that significantly different from the device **1**, which shows a blue emission around 440 nm from a pure TCIQ film. This indicates that the yellow EL arises from a CuI:TCIQ complex, consistent with the aforementioned PL study. Although the co-deposited CuI:TCIQ film showed similar PLQY (0.28) to that of the TCIQ film (0.22), the devices **2–4** have much higher efficiency than that of the device **1** (Figure 5d).

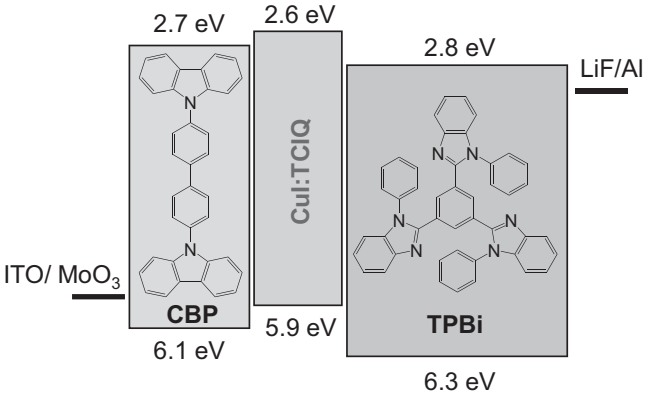

Figure 4. The schematic device structure, chemical structure, and energy level diagrams of the molecules used in OLEDs.

The higher efficiency is due to phosphorescent Cu(I) complex, which can harvest both singlet and triplet excitons, while TCIQ harvests only singlet excitons. By comparing the devices **2**, **3**, and **4**, it is found that the TCIQ based fluorescence peak disappears as the CuI doping concentration increasing from 1.0 wt% to 2.0 wt%. This is expected as a higher Cu(I) complex doping concentration would lead to a complete energy transfer from TCIQ to the Cu(I) complex. Among the four OLEDs, the best performance was observed in the device **4** with 5.0 wt% CuI. The turn-on voltage (V_{on}) and the maximum luminance (L_{max}) is 3.2 V and 7100 cd m^{-2}, and the maximum PE_{max} and CE_{max} are 10.2 lm W^{-1} and 10.4 cd A^{-1}, respectively, corresponding to a maximum EQE of 4.1% (**Table 3**).

It is interesting to note that the device **2** with a CuI doping concentration of 1.0 wt% showed both blue (440 nm) and yellow (580 nm) emissions. A combination of blue and yellow is the simplest method to fabricate WOLEDs. Considering the fact that the blue and yellow emissions are contributed from TCIQ and Cu(I) complex, respectively, and the proportion of blue emission in the device **2** is too small as compared to idea white emission, a series of OLEDs with CuI doping concentration below 1.0 wt% were constructed. In details, six devices with CuI doping concentration of 0.2 wt% (device **5**), 0.3 wt% (device **6**), 0.4 wt% (device **7**), 0.5 wt% (device **8**), 0.6 wt% (device **9**), and 0.7 wt% (device **10**), respectively, were fabricated.

Figure 6 shows EL spectra, *CD–V*, *L–V*, *CE–L*, *PE–L*, and *EQE–CD* characteristics of this set of OLEDs. As shown in the figure, the EL spectrum of the device can be easily tuned by changing the CuI doping concentration (Figure 6a), while it remains unchanged at different current densities (Figures S5 and S6, Supporting Information). As a result, an excellent white emission with a CIE of (0.30, 0.32) and a CRI of 89 was obtained in the device **5** at a CuI doping concentration of 0.2 wt% (Table 3). Meanwhile, the V_{on} and L_{max} of the device **5** is 3.5 V and 3886 cd m^{-2} (11 V), and the CE_{max} and EQE_{max} is 1.4 cd A^{-1} and 0.8%, respectively. Moreover, it is found that the efficiencies of devices **5–10** improves with the increasing of CuI doping concentration as shown in Figure 6d, which could be elucidated that the EQEs are mainly owing to the triplet harvesting portion. Considering that the device **5** showed the best white emission, the theoretical EQE limitation of our white OLEDs has been estimated based on the EL spectrum of the device **5**. It is found that the photon number ratio of the blue emission (arise from TCIQ) to yellow emission (arise from CuI:TCIQ) in the device **5** is about 1:2.6. Since the PLQYs of TCIQ and CuI:TCIQ films are 0.22 and 0.28, respectively. The theoretical maximum efficiency will be limited by the fluorescence from TCIQ, i.e., the maximum EQE of the blue emission is around 1.1%. Consequently, the device **5** may have a theoretical maximum EQE around 4.0%. The low EQE we obtained (0.8%) may arise from a poor singlet and triplet management within the device.

3. Conclusion

In this work, we report the synthesis, optical, thermal, and electrochemical properties of four compounds TCIQ, TCPy, 4CIQ, and CPy that containing pyridyl or isoquinolyl. Their neat and co-deposited CuI:L (L = TCIQ, TCPy, 4CIQ, or CPy)

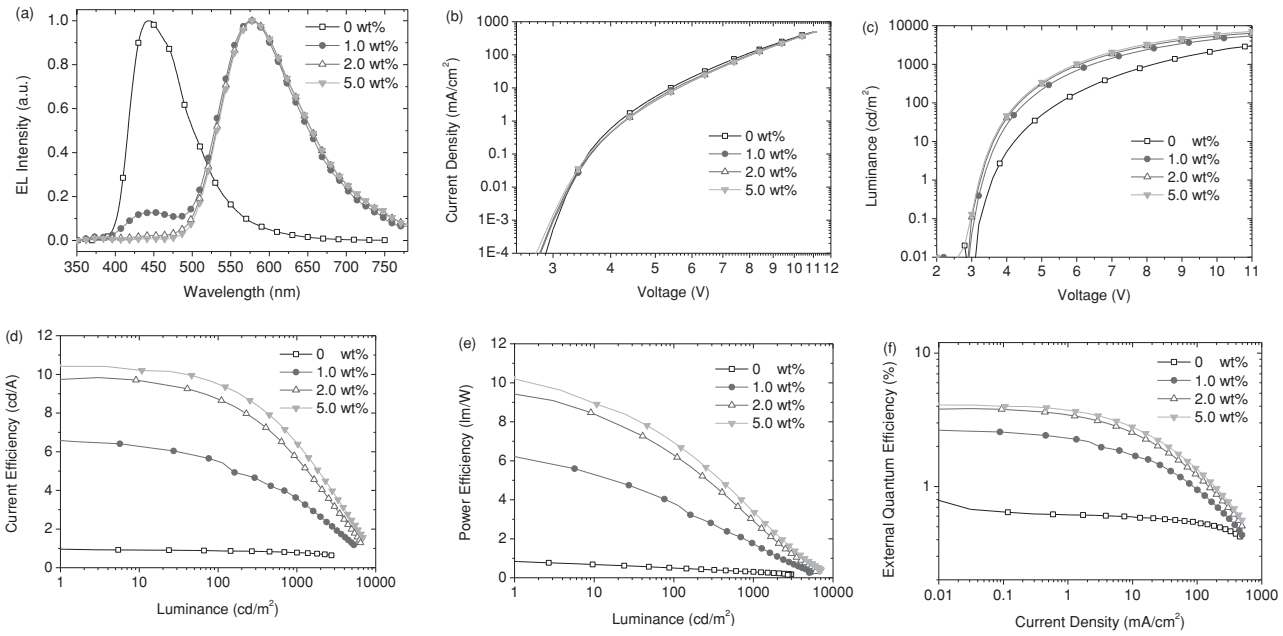

Figure 5. a) EL spectra, b) *CD–V*, c) *L–V*, d) *CE–L*, e) *PE–L*, and f) *EQE-CD* characteristics of devices **1–4** with configuration of ITO/MoO_3 (1 nm)/CBP (35 nm)/CuI:TCIQ (*x* wt%, 20 nm)/TPBi (65 nm)/LiF (1 nm)/ Al, where *x* = 0 (device **1**), 1.0 (device **2**), 2.0 (device **3**), and 5.0 (device **4**), respectively.

films at different CuI doping concentrations were photophysically studied. It is found that the CuI:TCIQ film shows pure yellow or white emission at different CuI doping concentrations, which attracts us to make simple yellow and white OLEDs. Consequently, a series of OLEDs with a device configuration of ITO/MoO_3 (1 nm)/CBP (35 nm)/CuI:TCIQ (20 nm)/TPBi (65 nm)/LiF (1 nm)/Al were fabricated. The best yellow OLED was achieved with a CuI doping concentration of 5 wt%, having maximum emission band at around 580 nm that arises from a in situ formed Cu(I) complex, while the WOLEDs were obtained with CuI doping concentration below 1.0 wt%, having transitions both from the Cu(I) complex and the compound TCIQ. Considering that TCIQ and CuI:TCIQ films showed moderate PLQYs as blue and yellow emitters, designing new compound that can function as efficient blue emitter, ligand, and host matrix, as well as distributing appropriately singlet and triplet excitons in OLEDs to balance an idea white EL spectrum and efficiency is in progress.

4. Experimental Section

General Information: All chemicals were used as received from commercial sources without further purification. ^{1}H-NMR spectra were recorded on a Varian-400M NMR spectrometer using DMSO-d_6 as the solvent. Chemical shift data for each signal were reported in ppm units with DMSO-d_6 as reference, where δ = 2.50. Mass spectra were measured on a Bruker Apex IV FTMS. Elemental analyses were performed on a VARIO EL analyzer (GmbH, Hanau, Germany).

Synthesis of CPy: A mixture of carbazole (7.35 g, 44 mmol), 3-bromopyridine (6.32 g, 40 mmol), potassium carbonate (6.07 g,

Table 3. Performance of OLEDs **1–10**.

Device	CuI conc. [%]	V_{on} [V]	L [cd m^{-2}]	CE [cd A^{-1}]	PE [lm W^{-1}]	EQE [%]	CRI	CIE [x, y]
1	0	3.6	2991	1.0	0.8	0.6	-	0.22, 0.24
2	1.0	3.3	5442	6.6	6.2	2.6	63	0.46, 0.46
3	2.0	3.3	6385	9.7	9.4	3.8	58	0.49, 0.49
4	5.0	3.2	7100	10.4	10.2	4.1	53	0.49, 0.49
5	0.2	3.5	3886	1.4	1.3	0.8	89	0.30, 0.32
6	0.3	3.4	4240	1.9	1.8	0.9	79	0.34, 0.36
7	0.4	3.4	4034	2.2	2.0	1.0	76	0.37, 0.38
8	0.5	3.4	4458	3.0	2.7	1.3	72	0.39, 0.40
9	0.6	3.3	4588	3.0	2.8	1.4	72	0.39, 0.40
10	0.7	3.3	4711	3.7	3.5	1.6	69	0.41, 0.43

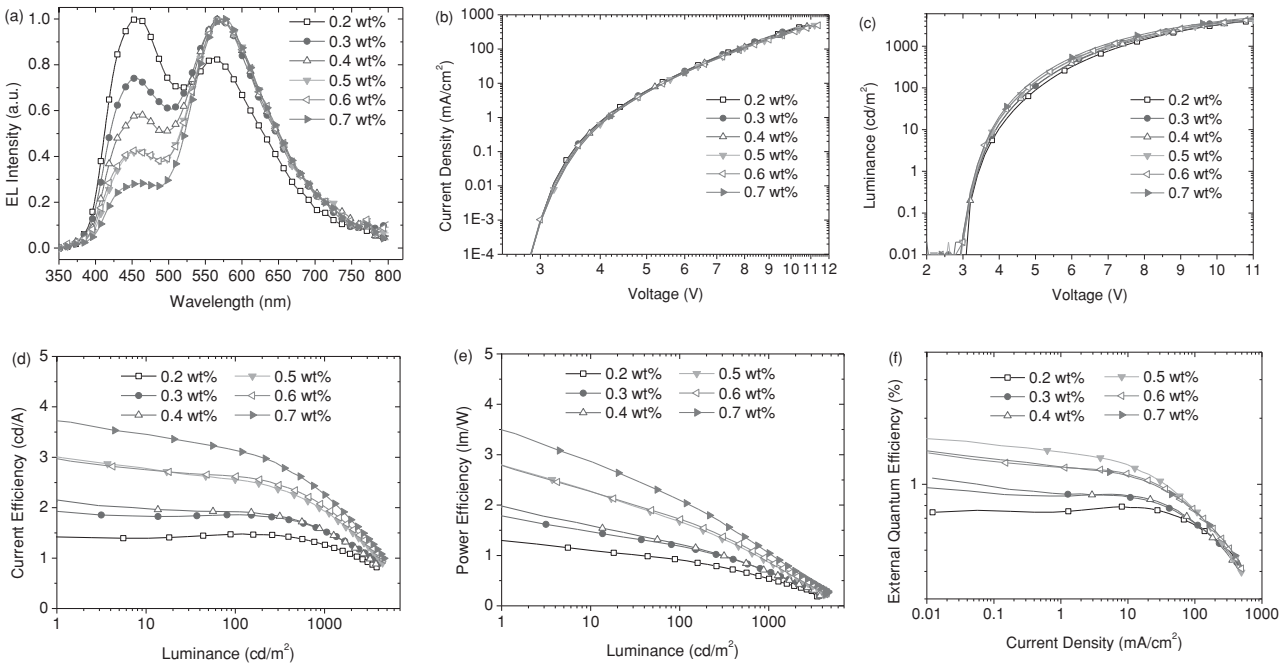

Figure 6. a) EL spectra, b) *CD–V*, c) *L–V*, d) *CE–L*, e) *PE–L*, and f) *EQE-CD* characteristics of devices **5–10** with the configuration of ITO/MoO_3 (1 nm)/CBP (35 nm)/CuI:TCIQ (*x* wt%, 20 nm)/TPBi (65 nm)/LiF (1 nm)/Al, where *x* = 0.2 (device **5**), 0.3 (device **6**), 0.4 (device **7**), 0.5 (device **8**), 0.6 (device **9**), and 0.7 (device **10**), respectively.

44 mmol), copper powder (2.00 g) and nitrobenzene (60 mL) was heated to 220 °C for 12 hrs. The mixture was then distilled at a reduced pressure. The obtained residue was extracted with CH_2Cl_2 and purified by column chromatography on silica gel to afford CPy (5.70 g, yield: 59%) as white solid. The compound was further purified by thermal gradient sublimation (190 °C–135 °C–50 °C) at low pressure (10^{-4} Pa). ^{1}H-NMR (400 MHz, DMSO-d_6, δ): 8.89 (s, 1H, pyridyl), 8.76 (s, 1H, pyridyl), 8.28 (s, 2H, carbazolyl), 8.13 (s, 1H, pyridyl), 7.73 (s, 1H, pyridyl), 7.45 (s, 2H, carbazolyl), 7.39 (s, 2H, carbazolyl), 7.32 (s, 2H, carbazolyl). EI-MS m/z: 245.1 (M+1). Anal. calcd. for $C_{17}H_{12}N_2$: C, 83.58; H, 4.95; N, 11.47. Found: C, 83.58; H, 4.97; N, 11.44.

Synthesis of Br$_2$CPy: To a solution of CPy (3.66 g, 15 mmol) in DMF (30 mL) at 0 °C was added NBS (5.87 g, 33 mmol). The solution was allowed to warm to room temperature and stirred overnight. After pouring into excess of water, the precipitation was collected by filtration, recrystallization from ethanol/CH_2Cl_2 to afford Br_2CPy (5.50 g, yield: 91%) as offwhite solid. ^{1}H-NMR (400 MHz, DMSO-d_6, δ): 8.88 (s, 1H, pyridyl), 8.78 (s, 1H, pyridyl), 8.61 (s, 2H, carbazolyl), 8.14 (s, 1H, pyridyl), 7.73 (d, 1H, pyridyl), 7.61(s, 2H, carbazolyl), 7.35 (s, 2H, carbazolyl). EI-MS m/z: 402.9 (M+1).

Synthesis of TCPy: A mixture of carbazole (2.75 g, 16.5 mmol), Br_2CPy (3.01 g, 7.5 mmol), potassium carbonate (2.27 g, 16.5 mmol), copper powder (1.00 g) and nitrobenzene (40 mL) was heated to 220 °C for 12 hrs. The mixture was then distillated at a reduced pressure. The obtained residue was extracted with CH_2Cl_2 and purified by column chromatography on silica gel to afford TCPy (2.85 g, yield: 66%) as white solid. The compound was further purified by thermal gradient sublimation (330 °C–265 °C–150 °C) at low pressure (10^{-4} Pa). ^{1}H-NMR (400 MHz, DMSO-d_6, δ): 9.12 (s, 1H, pyridyl), 8.86 (d, J = 3.6 Hz, 1H, pyridyl), 8.72 (s, 2H, carbazolyl), 8.37 (qq, J = 5.6 Hz, 1H, pyridyl), 8.26 (d, J = 6.0 Hz, 4H, carbazolyl), 7.84 (q, J = 10.4, 1H, pyridyl), 7.70 (m, 4H, carbazolyl), 7.42 (m, 8H, carbazolyl), 7.28 (m, 4H, carbazolyl). EI-MS m/z: 575.2 (M+1). Anal. calcd. for $C_{41}H_{26}N_4$: C, 85.69; H, 4.56; N, 9.75. Found: C, 85.73; H, 4.58; N, 9.74.

Synthesis of 4CIQ: The synthesis and work up process of 4CIQ is similar to that of CPy. Yield: 82%. The compound was further purified by thermal gradient sublimation (195 °C– 140 °C– 80 °C) at low pressure (10^{-4} Pa). ^{1}H-NMR (400 MHz, DMSO-d_6, δ): 9.60 (s, 1H, quinolyl), 8.76 (s, 1H, quinolyl), 8.39 (s, 1H, quinolyl), 8.32 (s, 2H, carbazolyl), 7.79 (s, 1H, quinolyl), 7.69 (s, 1H, quinolyl), 7.33 (m, 4H, carbazolyl), 7.05 (s, 1H, quinolyl), 6.97 (s, 2H, carbazolyl). EI-MS m/z: 295.1 (M+1). Anal. calcd. for $C_{21}H_{14}N_2$: C, 85.69; H, 4.79; N, 9.52. Found: C, 85.82; H, 4.83; N, 9.47.

Synthesis of Br$_2$CIQ: The synthesis and work up process of Br_2CIQ is similar to that of Br_2CPy. Yield: 85%. ^{1}H-NMR (400 MHz, DMSO-d_6, δ): 9.61 (s, 1H, quinolyl), 8.79 (s, 1H, quinolyl), 8.67 (s, 2H, carbazolyl), 8.40 (s, 1H, quinolyl), 7.80 (s, 1H, quinolyl), 7.71 (s, 1H, quinolyl), 7.52 (s, 2H, carbazolyl), 7.04 (s, 1H, quinolyl), 6.97 (s, 2H, carbazolyl). EI-MS m/z: 452.9 (M+1).

Synthesis of TCIQ: The synthesis and work up process of TCIQ is similar to that of TCPy. Yield: 74%. The compound was further purified by thermal gradient sublimation (350 °C– 285 °C– 150 °C) at low pressure (10^{-4} Pa). ^{1}H-NMR (400 MHz, DMSO-d_6, δ): 9.70 (s, 1H, quinolyl), 9.00 (s, 1H, quinolyl), 8.78 (s, 2H, carbazolyl), 8.48 (m, 1H, quinolyl), 8.26 (d, J = 6.0 Hz, 4H, carbazolyl), 7.88 (m, 2H, quinolyl), 7.62 (d, J = 6.8 Hz, 2H, carbazolyl), 7.43 (m, 9H, quinolyl and carbazolyl), 7.34 (d, J = 6.8 Hz, 2H, carbazolyl), 7.28 (m, 4H, carbazolyl). EI-MS m/z: 625.2 (M+1). Anal. calcd. for $C_{45}H_{28}N_4$: C, 86.51; H, 4.52; N, 8.97. Found: C, 86.59; H, 4.53; N, 8.93.

Photophysical Measurement: UV-Vis absorption spectra were recorded on a Shimadzu UV-3100 spectrometer. PL spectra were measured on an Edinburgh Analytical Instruments FLS920 spectrophotometer. PLQY was measured on Nanolog FL3–2iHR spectrometer with a integrating sphere. PL decay lifetimes were measured by time-correlated single photon counting using an IBH Fluorocube instrument equipped with a 331 nm LED excitation source.

Thermal Properties Measurements: Differential scanning calorimetry was performed on a Q600SDT instrument unit at a heating rate of 15 °C min^{-1} from 20 to 300 °C under nitrogen. The glass transition temperature was determined from the second heating scan. Thermogravimetric analysis was undertaken with a Q100DSC instrument. The thermal stability of the samples under a nitrogen atmosphere was determined by measuring their weight loss while heating at a rate of 15 °C min^{-1} from 25 to 600 °C.

Cyclic Voltammetry Measurements: Cyclic voltammetry was carried out in nitrogen-purged CH_2Cl_2 solution at room temperature with a CHI600C voltammetric analyzer and tetrabutylammonium hexafluorophosphate ($TBAPF_6$) (0.1 M) as the supporting electrolyte. The conventional three-electrode configuration is consists of a platinum working electrode, a platinum wire auxiliary electrode, and an Ag/AgCl wire pseudo-reference electrode.

OLED Fabrication and Measurements: The indium-tin oxide (ITO)-coated glass, hole injection material MoO_3, hole transporting material CBP, electron transporting material TPBi, and electron injection material LiF/Al were commercially available. In a general procedure, ITO-coated glass substrate was deposited with MoO_3 (1 nm) and then treated by ex situ UV ozone for 7 min. Then the sample was transferred to the deposition system. CBP (35 nm) was firstly deposited onto ITO/MoO_3 substrate, followed by emissive layer (20 nm), and TPBi (65 nm). Finally, a cathode composed of LiF (1 nm) and Al (100 nm) was sequentially deposited onto the substrate in another vacuum chamber (10^{-5} Pa). The luminance-current density-voltage (*L–I–V*) was measured using a HP4140B picoammeter and Minolta LS-110 luminance meter. The EL spectra were recorded using an USB2000-UV-vis Miniature Fiber Optic Spectrometer. All measurements were carried out in ambient atmosphere and at room temperature.

Supporting Information

Supporting Information of DFT calculations (Figure S1), thermogravimetric analysis curves (Figure S2), differential scanning calorimetry curves (Figure S3), cyclic voltammetry curves (Figure S4) of TCIQ, TCPy, 4CIQ, and CPy, and EL spectra of the OLEDs **5–10** at different current densities (Figures S5 and S6) is available from the Wiley Online Library or from the author.

Acknowledgements

We greatly acknowledge the financial support by The National Basic Research Program of China (No. 2006CB601103), The National Natural Science Foundation of China (NNSFC, Nos. 20971006, 90922004, 21201011), and The Specialized Research Fund for the Doctoral Program of Higher Education (20120001120116).

Received: February 28, 2014
Revised: April 14, 2014
Published online: June 24, 2014

[1] a) J. Kido, K. Hongawa, K. Okuyama, K. Nagai, *Appl. Phys. Lett.* **1994**, *64*, 815; b) Y. Z. Wang, R. G. Sun, F. Meghdadi, G. Leising, A. J. Epstein, *Appl. Phys. Lett.* **1999**, *74*, 3613.

[2] a) H. Kanno, R. J. Holmes, Y. Sun, S. Kena-Cohen, S. R. Forrest, *Adv. Mater.* **2006**, *18*, 339; d) S. Mladenovski, K. Neyts, D. Pavicic, A. Werner, C. Rothe, *Opt. Express* **2009**, *17*, 7562.

[3] a) J. Kalinowski, M. Cocchi, D. Virgili, V. Fattori, J. A. G. Williams, *Adv. Mater.* **2007**, *19*, 4000; b) E. L. Williams, K. Haavisto, J. Li, G. E. Jabbour, *Adv. Mater.* **2007**, *19*, 197; c) B. W. D'Andrade, J. Brooks, V. Adamovich, M. E. Thompson, S. R. Forrest, *Adv. Mater.* **2002**, *14*, 1032.

[4] a) B. C. Krummacher, V. E. Choong, M. K. Mathai, S. A. Choulis, F. So, F. Jermann, T. Fiedler, M. Zachau, *Appl. Phys. Lett.* **2006**, *88*, 113506; b) V. Gohri, S. Hofmann, S. Reineke, T. Rosenow, M. Thomschke, M. Levichkova, B. Lussem, K. Leo, *Org. Electron.* **2011**, *12*, 2126.

[5] a) B. W. D'Andrade, R. J. Holmes, S. R. Forrest, *Adv. Mater.* **2004**, *16*, 624; b) J. Liu, Q. G. Zhou, Y. X. Cheng, Y. H. Geng, L. X. Wang, D. G. Ma, X. B. Jing, F. S. Wang, *Adv. Mater.* **2005**, *17*, 2974.

[6] a) S. Reineke, F. Lindner, G. Schwartz, N. Seidler, K. Walzer, B. Lussem, K. Leo, *Nature* **2009**, *459*, 234; b) J. Kido, M. Kimura, K. Nagai, *Science* **1995**, *267*, 1332.

[7] a) Y. R. Sun, N. C. Giebink, H. Kanno, B. W. Ma, M. E. Thompson, S. R. Forrest, *Nature* **2006**, *440*, 908; b) G. Schwartz, M. Pfeiffer, S. Reineke, K. Walzer, K. Leo, *Adv. Mater.* **2007**, *19*, 3672; c) B. P. Yan, C. C. C. Cheung, S. C. F. Kui, H. F. Xiang, V. A. L. Roy, S. J. Xu, C. M. Che, *Adv. Mater.* **2007**, *19*, 3599.

[8] a) L. X. Xiao, Z. J. Chen, B. Qu, J. X. Luo, S. Kong, Q. H. Gong, J. J. Kido, *Adv. Mater.* **2011**, *23*, 926; b) Y. T. Tao, C. L. Yang, J. G. Qin, *Chem. Soc. Rev.* **2011**, *40*, 2943; c) Y. Shirota, H. Kageyama, *Chem. Rev.* **2007**, *107*, 953; d) J. A. G. Williams, S. Develay, D. L. Rochester, L. Murphy, *Coord. Chem. Rev.* **2008**, *252*, 2596; e) Z. W. Liu, Z. Q. Bian, C. H. Huang, *Top. Organomet. Chem.* **2010**, *28*, 113.

[9] a) P. C. Ford, E. Cariati, J. Bourassa, *Chem. Rev.* **1999**, *99*, 3625; b) N. Armaroli, G. Accorsi, F. Cardinali, A. Listorti, *Top. Curr. Chem.* **2007**, *280*, 69; c) D. V. Scaltrito, D. W. Thompson, J. A. O'Callaghan, G. J. Meyer, *Coord. Chem. Rev.* **2000**, *208*, 243; d) D. R. McMillin, K. M. McNett, *Chem. Rev.* **1998**, *98*, 1201.

[10] a) Z. B. Wang, M. G. Helander, J. Qiu, D. P. Puzzo, M. T. Greiner, Z. M. Hudson, S. Wang, Z. W. Liu, Z. H. Lu, *Nat. Photonics* **2011**, *5*, 753; b) M. G. Helander, Z. B. Wang, J. Qiu, M. T. Greiner, D. P. Puzzo, Z. W. Liu, Z. H. Lu, *Science* **2011**, *332*, 944.

[11] a) O. Horvath, *Coord. Chem. Rev.* **1994**, *135*, 303; b) C. Kutal, *Coord. Chem. Rev.* **1990**, *99*, 213; c) C. Vogler, H. D. Hausen, W. Kaim, S. Kohlmann, H. E. A. Kramer, J. Rieker, *Angew. Chem. Int. Ed.* **1989**, *28*, 1659.

[12] a) S. B. Harkins, J. C. Peters, *J. Am. Chem. Soc.* **2005**, *127*, 2030; b) D. G. Cuttell, S. M. Kuang, P. E. Fanwick, D. R. McMillin, R. A. Walton, *J. Am. Chem. Soc.* **2002**, *124*, 6; c) D. M. Zink, M. Bachle, T. Baumann, M. Nieger, M. Kuhn, C. Wang, W. Klopper, U. Monkowius, T. Hofbeck, H. Yersin, S. Brase, *Inorg. Chem.* **2013**, *52*, 2292; d) J. C. Deaton, S. C. Switalski, D. Y. Kondakov, R. H. Young, T. D. Pawlik, D. J. Giesen, S. B. Harkins, A. J. M. Miller, S. F. Mickenberg, J. C. Peters, *J. Am. Chem. Soc.* **2010**, *132*, 9499; e) Q. S. Zhang, T. Komino, S. P. Huang, S. Matsunami, K. Goushi, C. Adachi, *Adv. Funct. Mater.* **2012**, *22*, 2327; f) M. Hashimoto, S. Igawa, M. Yashima, I. Kawata, M. Hoshino, M. Osawa, *J. Am. Chem. Soc.* **2011**, *133*, 10348.

[13] a) K. R. Kyle, C. K. Ryu, J. A. Dibenedetto, P. C. Ford, *J. Am. Chem. Soc.* **1991**, *113*, 2954; b) T. H. Kim, Y. W. Shin, J. H. Jung, J. S. Kim, J. Kim, *Angew. Chem. Int. Ed.* **2008**, *47*, 685.

[14] Z. W. Liu, M. F. Qayyum, C. Wu, M. T. Whited, P. I. Djurovich, K. O. Hodgson, B. Hedman, E. I. Solomon, M. E. Thompson, *J. Am. Chem. Soc.* **2011**, *133*, 3700.

[15] S. L. Gong, X. He, Y. H. Chen, Z. Q. Jiang, C. Zhong, D. G. Ma, J. G. Qin, C. L. Yang, *J. Mater. Chem.* **2012**, *22*, 2894.

[16] W. Jiang, L. A. Duan, J. A. Qiao, G. F. Dong, D. Q. Zhang, L. D. Wang, Y. Qiu, *J. Mater. Chem.* **2011**, *21*, 4918.

[17] M. H. Tsai, Y. H. Hong, C. H. Chang, H. C. Su, C. C. Wu, A. Matoliukstyte, J. Simokaitiene, S. Grigalevicius, J. V. Grazulevicius, C. P. Hsu, *Adv. Mater.* **2007**, *19*, 862.

[18] W. Jiang, L. A. Duan, J. Qiao, D. Q. Zhang, G. F. Dong, L. D. Wang, Y. Qiu, *J. Mater. Chem.* **2010**, *20*, 6131.

[19] B. W. D'Andrade, S. Datta, S. R. Forrest, P. Djurovich, E. Polikarpov, M. E. Thompson, *Org. Electron.* **2005**, *6*, 11.

[20] F. De Angelis, S. Fantacci, A. Sgamellotti, E. Cariati, R. Ugo, P. C. Ford, *Inorg. Chem.* **2006**, *45*, 10576.